



Instrumental Developments

(BL2B1)

Fourth electron-ion coincidence spectroscopy adapting a Siegbahn-type coaxially symmetric electron energy analyzer

Koji Isari, Kenichiro Tanaka, Kazuhiko Mase,^A Shin-ichi Nagaoka,^B

Department of Physics Science, Faculty of Science, Hiroshima University, 1-3-1 Kagamiyama, Higashi-Hiroshima 739-8527

^A*Photon Factory, Institute of Materials Structure Science, High Energy Accelerator Research Organization, 1-1 Oho, Tsukuba 305-0801*

^B*Institute for Molecular Science, Myodaiji Okazaki 444-8585*

Energy-selected electron ion coincidence (EICO) spectroscopy is an ideal tool for investigations of the ion desorption mechanism induced by electronic transitions, because it provides mass spectra for the ion desorption channels related to the selected electron transitions [1]. One of the authors has developed three EICO analyzers at BL-2B1 for the study of surface dynamics so far [2]. To achieve a fair signal-to-background ratio, the solid angles of the electron energy analyzer and the time-of-flight mass spectrometer (TOF-MS) have been improved. In the present article, we report the design of the fourth EICO analyzer. The EICO analyzer is constructed on a 203-mm-diameter conflat flange as a bolt-on instrument, which consists of a Siegbahn-type coaxially symmetric mirror electron energy analyzer [3] for detection of energy-resolved electrons, a TOF-MS for ion detection and an xyz stage for position adjustment. Figure 1 shows a photograph of the fourth EICO apparatus. The solid angle of the electron energy analyzer (1.2 sr) is designed to achieve a fair signal-to-background ratio within a reasonable data collection time. The TOF-MS is located coaxially to the electron energy analyzer. The surface normal of sample is set coaxially to the electron energy analyzer and the TOF-MS. The performance of the electron energy analyzer was examined at BL-2B1. The sample was a gold film without surface cleaning. The electron states of the surface were excited by *p*-polarized radiation with an incident angle of 60° with respect to the surface normal. The base pressure was 1.8×10^{-10} Torr. Figure 2 shows the photoelectron spectrum at $h\nu = 350$ eV in Au 4f region. Based on Gaussian curve fitting the energy resolution was estimated to be $E/\Delta E = 130$ at the $4f_{7/2}$ peak, full width at half maximum (FWHM) of which was 2.0 eV.

References

- [1] K. Mase *et al.*, *J. Electron Spectros. Relat. Phenom.* **101-103**, 13 (1999).
- [2] K. Mase *et al.*, *UVSOR ACTIVITY REPORT 1999*, 35 (2000).
- [3] K. Siegbahn *et al.*, *Nucl. Instr. and Meth. in Phys. Res.* **A384**, 563-574 (1997).

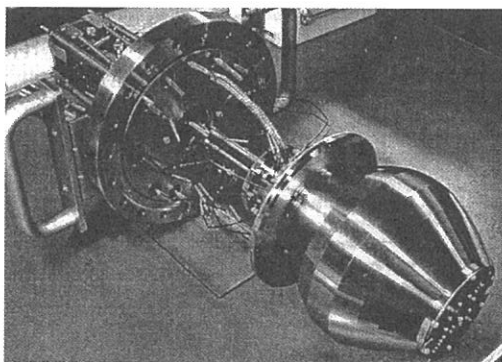


Figure 1. Photograph of the fourth EICO analyzer.

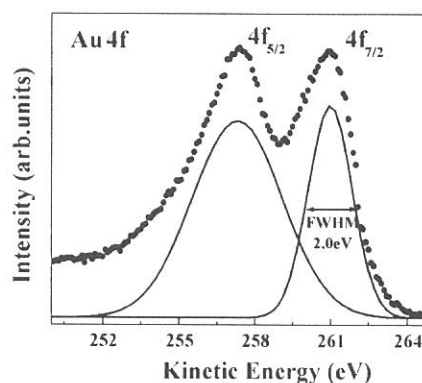


Figure 2. Au 4f photoelectron spectrum taken at a photon energy of 350 eV with the Siegbahn-type coaxially symmetric mirror electron energy analyzer.

(BL2A)

Development and evaluation of a video-microscope-computer system for observation and analyses of behavioral responses of microorganisms to ultraviolet light from the synchrotron radiation light source

Shigeru Matsunaga¹, Terumitsu Hori¹, Sho-ichi Higashi², Shinji Ito^{2,3}, Tetsuo Takahashi⁴, Yasutaka Takata⁵, Takaki Hatsui⁵, Nobuhiro Kosugi⁵ and Masakatsu Watanabe^{2,3}

¹Institute of Biological Sciences, University of Tsukuba, Tsukuba 305-8532; ²National Institute for Basic Biology, Okazaki 444-8585; ³Department of Photoscience, School of Advanced Sciences, Graduate University for Advanced Studies, Hayama 240-0193; ⁴Japan Advanced Institute for Science and Technology, Tatsunokuchi 923-1292; ⁵Institute for Molecular Science, Okazaki 444-8585

Single-celled microorganisms such as cyanobacteria, halophilic archaea (formerly called archaeobacteria) and unicellular flagellate algae show behavioral responses to visible and UV light so that they can accumulate in suitable or avoid harmful light conditions (e. g.[1-4]). Because they originated in Precambrian era, much before the establishment of the stratospheric ozone layer, they must have had, thus may well even now have, sensitive behavioral responses to avoid shorter-wavelength UV (e. g. 220-300 nm), than the present-day terrestrial UV (of wavelengths longer than ca. 300 nm because of the ozone layer). Indeed, we have demonstrated that the unicellular flagellate alga *Euglena* ("Midorimushi" in Japanese) cells do show clear photoavoidance as well as photoaccumulation responses even at 280 nm [3]. It is therefore interesting and meaningful to extend such wavelength-dependency studies into shorter wavelength regions of UV, artificially obtainable from the synchrotron radiation, in order to understand bio-molecular mechanisms as well as ecological and evolutionary significance of the short-wavelength-UV-sensing in such microorganisms.

Preliminary measurement with calibrated Si photodiodes indicated that the maximum monochromatic UV light fluence rate at BL2A of UVSOR at 200 nm at the ring current of 180 mA is ca. 2×10^{10} photons/mm²/s (ca. 0.03 μ mole/m²/s), which is 1 order of magnitude lower than that needed to induce the behavioral responses of *Euglena* cells [5]. Therefore a quartz lens was mounted on the optical axis to condense the monochromatic UV light on to the sample suspension in a quartz chamber on the stage of a microscope connected to a CCD camera (Fig. 1a, b). Slantly projected observation light beam from a microscopic projector was usually filtered through an infrared- or a red-transmitting filter before reaching the sample. The images of the *Euglena* cells were recorded at the video-rate of 30 frames/s using a video-recorder and were thereafter analysed on a Macintosh computer using the public domain NIH Image program (developed at the U.S. National Institutes of Health and available on the Internet at <http://rsb.info.nih.gov/nih-image/>).

By using the above-described system, we have succeeded in detecting the behavioral responses of the *Euglena* cells to avoid the monochromatic UV light of 220 nm in wavelength: Fig. 2 shows that the cells avoid the central round area which is irradiated with the 220 nm UV light condensed by the quartz lens. After some more refinement of the system especially in terms of microscopic-scale positional reproducibility and numerical quantification of the behavioral responses, extensive experiments on wavelength- and fluence-rate-dependency of the behavioral responses in various microorganisms will become possible.

Acknowledgements

We thank Profs. Toshio Ibuki (Kyoto University of Education), Kazumichi Nakagawa (Kobe University), Kotaro Hieda (Rikkyo University) and Mr. Mamoru Kubota (National Institute for Basic Biology) for their advice and help in measurement of fluence rates of the monochromatic UV light at BL2A. Shigeru Matsunaga acknowledges support from Technology Department of IMS under the Technical Staff Training Program.

References

- [1] Choi, J.-S., Chung, Y.-H., Moon, Y.-J., Kim, C., Watanabe, M., Song, P.-S., Joe, C.-O., Bogorad, L. and Park, Y. M.: *Photochem. Photobiol.* 70, 95-102 (1999).
- [2] Takahashi, T., Yan, B., Mazur, P., Derguini, F., Nakanishi, K. and Spudich, J. L.: *Biochem.* 29, 8467-8474 (1990).
- [3] Matsunaga, S., Hori, T., Takahashi, T., Kubota, M., Watanabe, M., Okamoto, K., Masuda, K. and Sugai, M.: *Protoplasma* 201, 45-52 (1998).
- [4] Watanabe, M.: In *CRC Handbook of Organic Photochemistry and Photobiology*. pp. 1276-1288 (1995).
- [5] Matsunaga, S.: Doctoral Thesis, Univ. Tsukuba (1999).

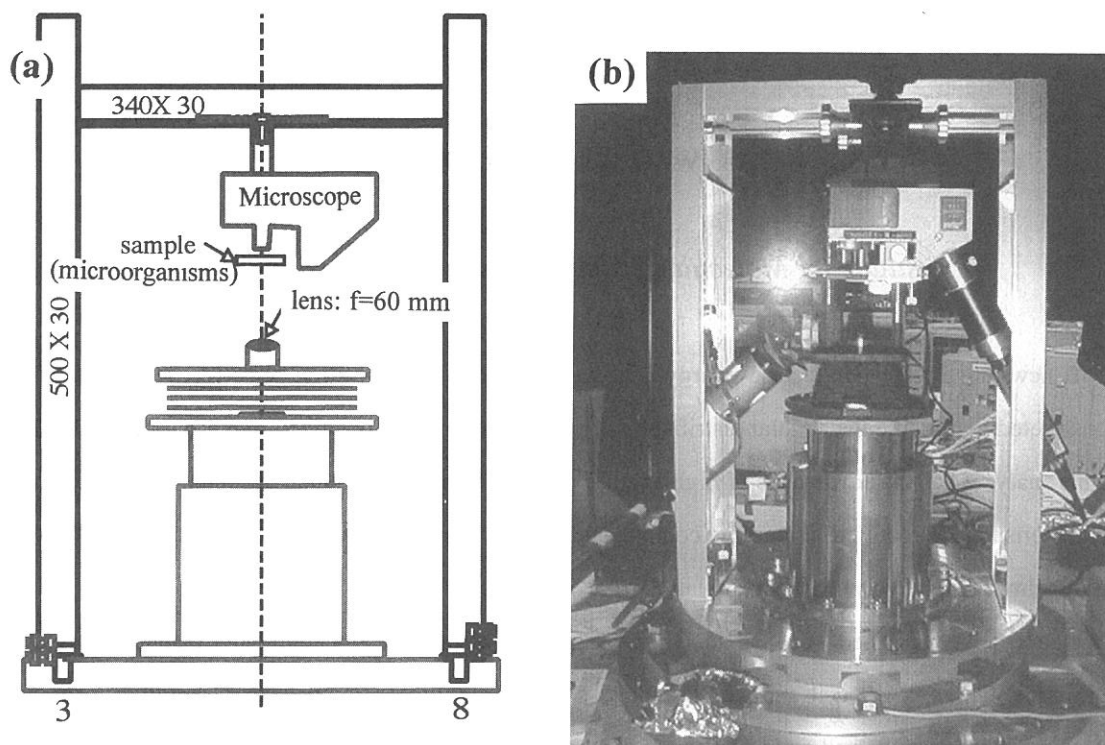


Fig. 1 a, b. Schematic layout (a) and photograph (b) of the video-microscopic system for observation of behavioral responses of microorganisms to monochromatic UV light from BL2A of UVSOR. The UV light beam is projected vertical-upwardly.

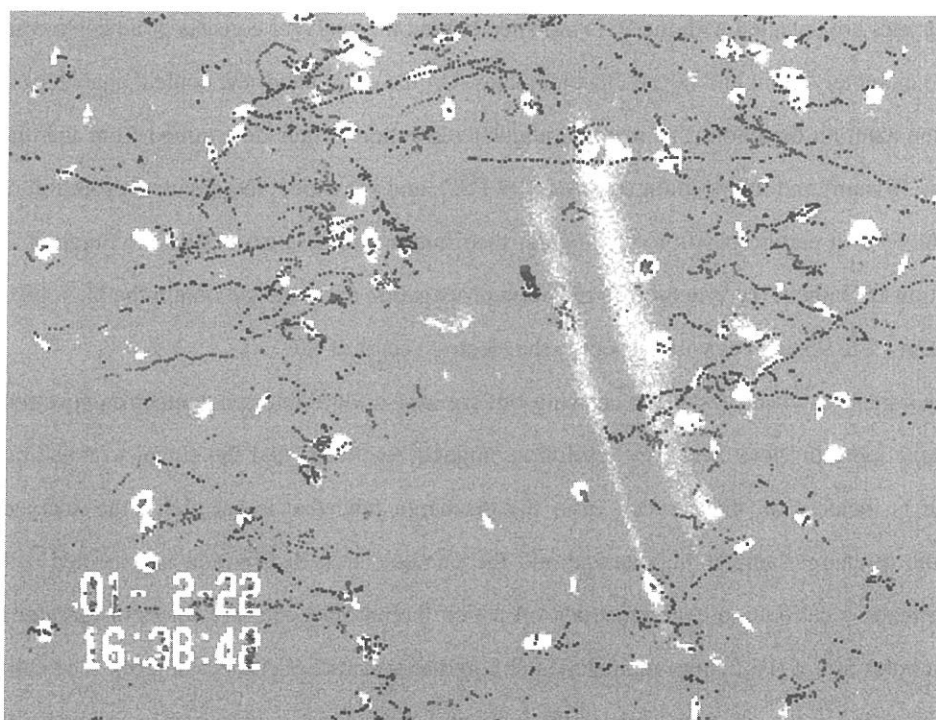


Fig. 2. Swimming tracks, in 8 s, of *Euglena* ("Midorimushi" in Japanese) cells. The cells are avoiding the central round area irradiated with monochromatic UV light of 220 nm in wavelength.

(BL-3B)

Construction of a conical energy analyzer for angle-resolved photoelectron spectroscopy

Kota IWASAKI and Koichiro MITSUKE

Institute for Molecular Science, Myodaiji, Okazaki 444-8585, Japan

A new angle-resolved electron energy analyzer incorporating a position sensitive detector (PSD) has been constructed to measure the angular distribution of photoelectron from polarized rare gas atoms in BL3B.

This analyzer has the advantages of high angular resolution and wide angular acceptance simultaneously. These characteristics are required to measure complicated angular distributions of photoelectrons caused by the atomic alignment with relatively short accumulation time of signals.

We have newly designed a conical analyzer consisting of a set of an inner and outer conical deflector electrode, cylindrical lenses, a gas cell and a PSD unit as shown in Figure 1. Photoelectrons emitted in the gas cell are accelerated between the cell and an extractor electrode, then focused on an entrance slit by the cylindrical lenses. The electron trajectories between the inner and the outer conical electrodes are similar to those expected for a conventional parallel-plate analyzer. However, the conical analyzer has considerably larger energy dispersion and larger angular aberration than the parallel-plate analyzer. Energy selected electrons exiting out of the conical deflector electrodes are detected with the PSD mounted behind the analyzer consists of a resistive anode encoder of an effective diameter 40mm and micro-channel plates. On the other hand, the conical analyzer is incapable of focussing in the azimuth direction. The azimuth angular resolution is thus determined from the diameter of the sample volume (ϕ 1mm) and the position sensitivity of PSD, and we expect the angular resolution of 1.5 degree. With fixing the PSD at certain position, the angular distribution can be measured in the range of 25 degrees at once. By rotating PSD about the synchrotron radiation propagation axis, we can obtain the photoelectron angular distribution from -5 to 95 degrees with respect to the electric vector of SR.

Our analyzer system has been tested by carrying out gas phase ultraviolet photoelectron spectroscopy with a helium discharge lamp in view of energy resolution, angular resolution and the signal to noise ratio. The HeI (58.4nm) light is incident on the gas cell from the discharge tube that is set above the analyzer. The light produced in the discharge lamp is unpolarized and the photoelectron distribution is expected to be isotropic. Therefore, we made a calibration cone electrode on which the entrance slit is a series of circular holes as test objects. These holes are of 0.5-2.0mm diameters and bored at intervals of 4.5-8.5 degrees. The calibration cone electrode was installed in the analyzer to check the focussing characteristics by observing photoelectrons passing through the circular holes.

In the first stage of the performance test, extremely high background due to low energy electrons was a serious problem. We have measured the dependence of the rate of the background on the transmission energy, deceleration energy of cylindrical lens and the Ar gas pressure to examine the origin of background electrons. The result showed that the background signals are caused by the photoelectrons emitted from the metal surfaces near the gas cell.

We have therefore tried to prevent the photoelectrons from entering the detector by setting a photoelectron shield applied at a potential of 20V. Consequently, the background signals have been suppressed to about 1/100 comparing to those before the improvement. The following performance test is being carried out.

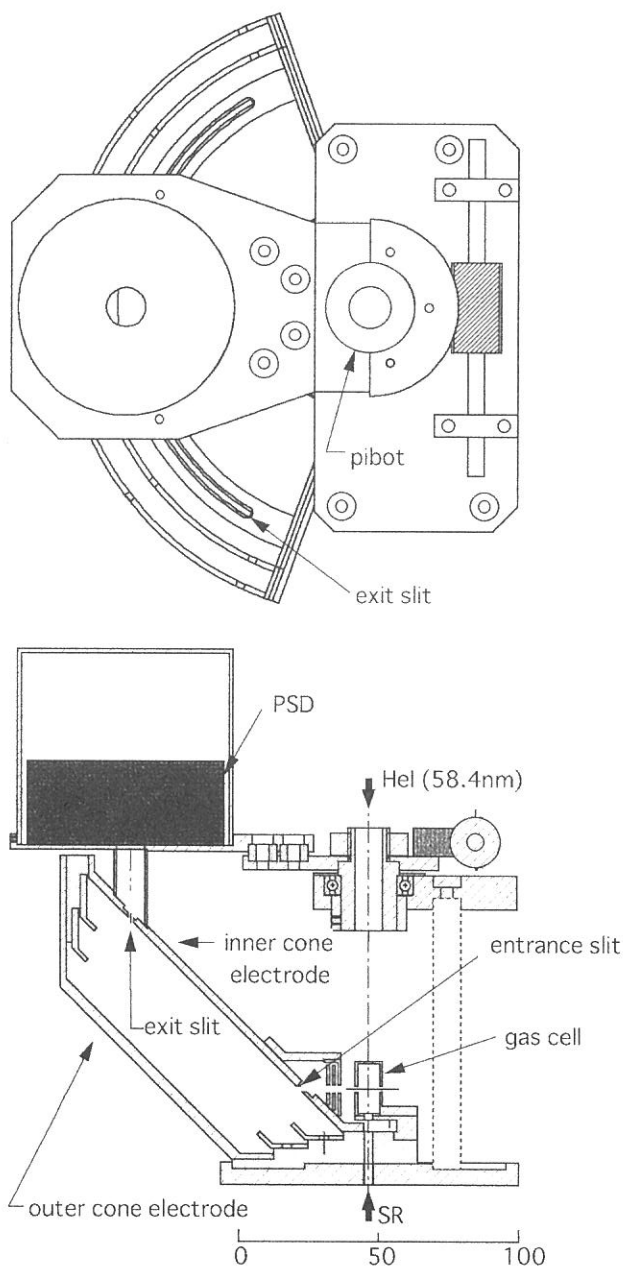


Figure 1. Schematic diagram of the conical analyzer. Synchrotron radiation is introduced in the gas cell through a plate holding all the electrodes and Hel light is so as to counterpropagate the SR.

Reconstruction of BL4A Beam Line and Infrared Reflection Absorption Spectroscopy System

Zhihong Wang¹, Hideyuki Noda¹, Youichi Nonogaki² and Tsuneo Urisu^{1,2}

(¹The Graduate University for Advanced Studies, ²Institute for Molecular Science)

Re-arrangement of the beam line at BL4A has already started this year. Now it is still under construction. The IRRAS(Infrared Reflection Absorption Spectroscopy) system has been moved from BL4B to BL4A2. The reaction gas lines have been reconstructed connecting with new interlock system. The reaction chamber for IRRAS measurement was also reconstructed. The new system only use one chamber instead of formal two for the sample transfer to the measurement chamber to make the transfer more easy and efficient. The interlock system connecting these chambers and turbo molecular pumps also has been changed to the more simple and practical one.

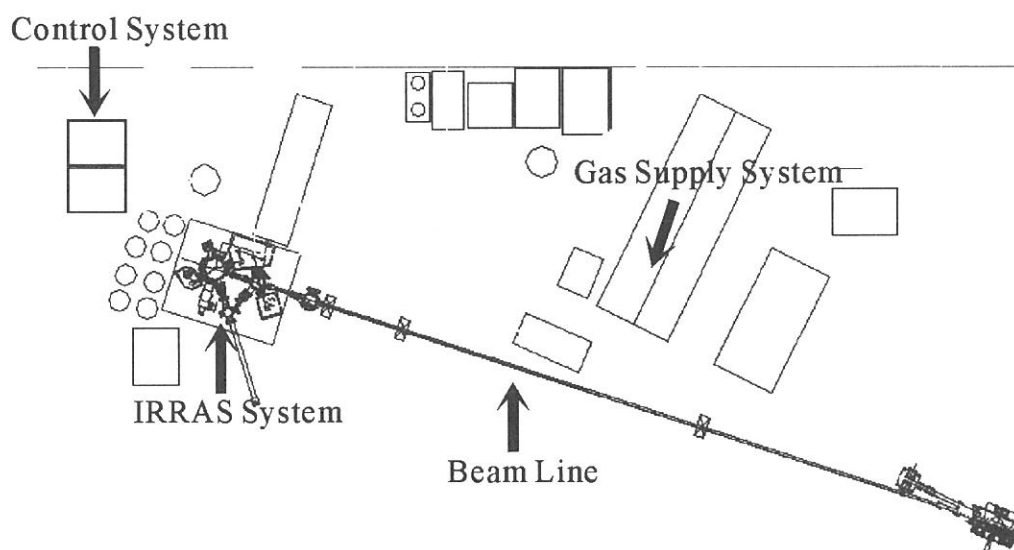


Figure 1 BL4A2 and IRRAS system after reconstruction

(BL6B)

Construction of BL6B for UHV-STM Observation of Si Surfaces Irradiated by Synchrotron Radiation

Y. Nonogaki, Y. Gao^a, H. Noda, Z. Wang, T. Urisu

Institute for Molecular Science, Myodaiji, Okazaki, 444-8585, Japan

^a*The Graduate University for Advanced Studies, Myodaiji, Okazaki, 444-8585, Japan*

Synchrotron radiation (SR) processing including selective cleaving of chemical bonds through the tunability of the photon energy by exciting certain dissociative energy levels, has advantages of lower damage in comparison to plasma processes, high spatial resolution and aspect ratio because of the shorter wavelengths, and the applicability to thick insulating materials where nanofabrication techniques based on charged particles such as electron beam lithography cannot be used.

STM observations are important for investigation of the SR illumination effect on Si surface for surface photochemistry and semiconductor technology for nanostructure fabrication. Our group has reported the SR stimulated cleaning of Si (111) by using BL4B in UVSOR[1-3]. In a pure thermal cleaning, the Si wafer had to be heated to $> 850^{\circ}\text{C}$ and, additional long hours of annealing at 700°C was required to obtain the thermal equilibrium surface. In a SR stimulated cleaning, on the other hand, the desorption of SiO_2 occurred at much lower temperatures ($650\text{-}700^{\circ}\text{C}$) and atomically flat surfaces free of voids, which inevitably appeared in a pure thermal desorption at these low temperatures, were observed.

We also found an interesting nanostructure formed on Si (111) surface by SR stimulated cleaning. At upper right corner in Fig. 1 a strip terrace of which width quantized to the units of 7×7 unit cell were observed. It shows that the steps align along the boundaries of the 7×7 unit cell. We think combination of the SR stimulated cleaning and a vicinal surface realize an ordered structure on the surface with the straight steps separated by the width quantized terraces. Now we are preparing to investigate surface misorientation effects on step alignment.

In last year, we moved all the BL4B beam line components into BL6B and reconstructed them. The base pressures achieved now at the pre-mirror and beam line are $\sim 1\times 10^{-9}$ Torr and $\sim 3\times 10^{-9}$ Torr, respectively. However, the vacuums, introducing SR light into beam line, become worse due to the degas from mirror and beam line itself. We are now drying beam line components.

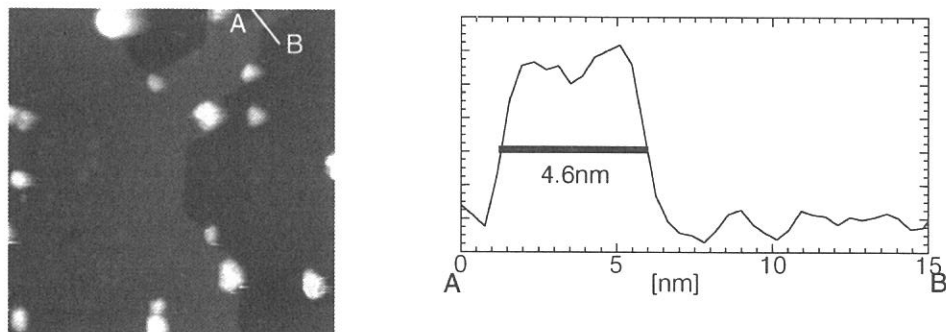


Figure 1: 100 nm x 100 nm STM topograph and line profile across the stripe at the upper-right-hand side corner. The sample is a Si (111) substrate after 5 h of SR irradiation at 650°C .

[1] T. Miyamae, H. Uchida, I.H. Munro and T. Urisu, *J. Vac. Sci. Technol.* A18, 1 (1999).

[2] Y. Gao, H. Mekaru, T. Miyamae and T. Urisu, *Appl. Phys. Lett.* 76, 1392 (2000).

[3] Y. Gao, H. Mekaru, T. Miyamae and T. Urisu, *J. Vac. Sci. Technol. A* 18, 1053 (2000).

(BL4B)

The first performance tests for a new monochromator on BL4B

Eiji Shigemasa, Tatsuo Gejo, Naonori Kondo, Hiroshi Oji, Mitsuru Nagasono, Takaki Hatsui,
and Nobuhiro Kosugi

Institute for Molecular Science, Okazaki 444-8585, JAPAN

In order to realize various studies on vibrational spectroscopy in the soft x-ray range (100 ~ 1000 eV), which contains the *K*-shell thresholds of chemically important elements like C, N, and O, the construction of a new grazing incidence monochromator on BL4B at the UVSOR has begun. The Varied-line-spacing Plane Grating Monochromator (VPGM) has been chosen for this work [1] and its installation has been successfully finished in October 2000. The vacuum condition was ready for obtaining the first SR light until the end of December 2000, and the first performance tests for the monochromator have just been started.

The absolute photon flux for two gratings available so far (267 and 800 l/mm) has been measured using a Si photodiode supplied by IRD Inc. With the entrance and exit slit openings set at 25 and 10 μm , corresponding to the resolving power of 10000 at 400 eV with the 800 l/mm grating, the photocurrent from the photodiode was measured after the sample position, and converted into the absolute photon flux, taking account of the quantum efficiency of the photodiode. In this case, the resolving power in the regular spectral region for each grating is more than 3000. The throughput photon flux measured ranges from 10^8 to 10^9 photons/sec for the ring current of 100 mA, which is a little smaller than that estimated.

The inner-shell photoabsorption spectra of Ar and N_2 were measured, to demonstrate the instrumental resolution. The *K*-shell photoabsorption spectrum of N_2 at the $\text{N } 1s \rightarrow \pi^*$ resonance is presented in Fig. 1. The entrance and exit slits were set for achieving the resolving power of 10000. From the comparison with all available spectra of the $\text{N } 1s \rightarrow \pi^*$ resonance of N_2 , it seems to be reasonable that the resolving power obtained here is more than 5000. The photoabsorption spectrum in the vicinity of the 2p ionization thresholds of Ar (~250 eV) was also recorded using the 800 l/mm grating, with slit openings of 50 and 10 μm , for the entrance and exit slits, respectively. The Ar $2p \rightarrow nd$ Rydberg series up to $n=7$ are observed. This implies that the resolving power is more than 8000 at this photon energy region, and is in good accord with the theoretically predicted value.

To improve the total throughput of the monochromator, further fine tunings for all optical elements through the performance tests is obviously necessary. Experiments for angle-resolved photoion spectroscopy and photoelectron spectroscopy in a gas phase are expected to be started in the near future.

Reference

[1] Y. Takata, T. Gejo, and E. Shigemasa, UVSOR Activity Report 1999, p. 42.

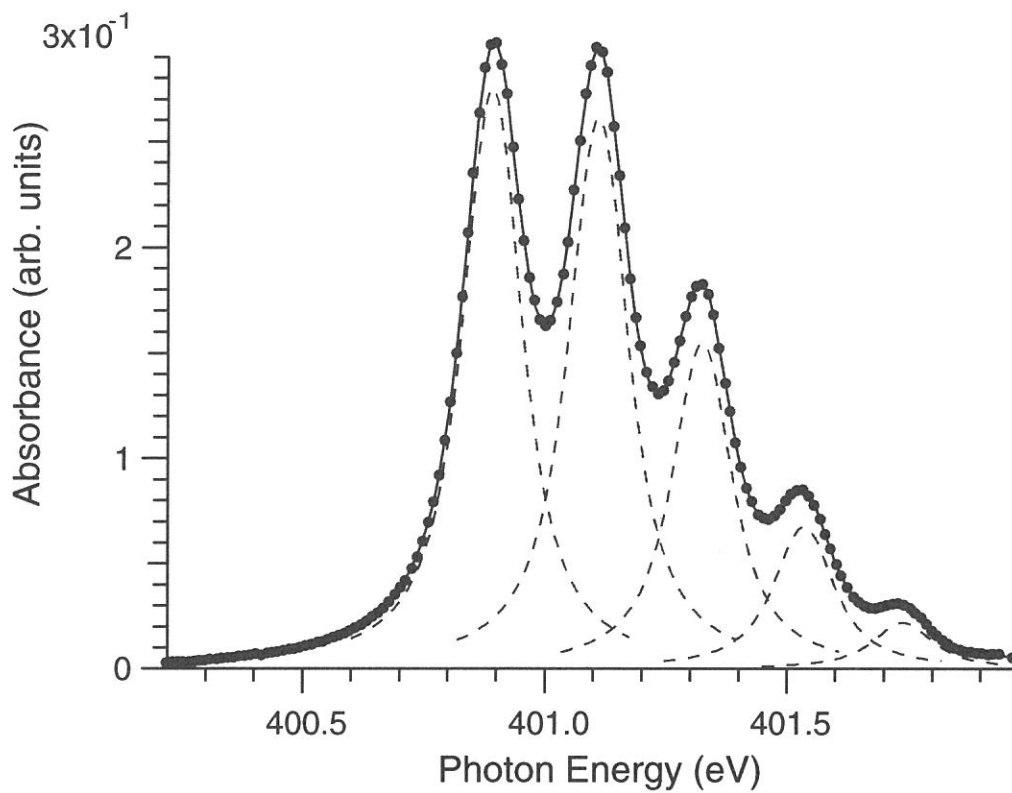


Figure 1. K -shell photoabsorption spectrum of N_2 at the $N\ 1s \rightarrow \pi^*$ resonance.

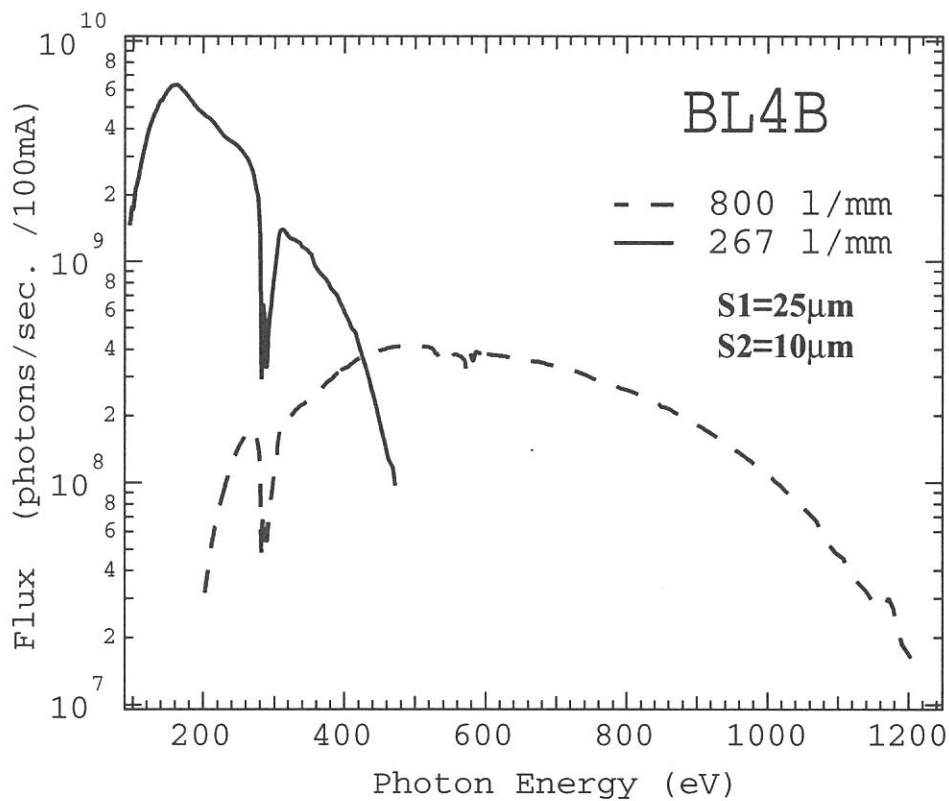


Figure 2. Absolute photon flux measured by a Si photodiode.

(BL4B)

The Resolving Power of the New Monochromator at BL4B

Mitsuru Nagasono, Eiji Shigemasa, Tatsuo Gejo, Hiroshi Oji, Takaki Hatsui,
and Nobuhiro Kosugi

Institute for Molecular Science, Okazaki 444-8585, JAPAN

Resolution is an important index for the performance of monochromators. In order to demonstrate the instrumental resolution, the inner-shell photoabsorption spectra of N_2 and O_2 were measured with the grating having the groove density of 800 l/mm.

The resolving power dependences of the K -shell photoabsorption spectra of N_2 at the $N\ 1s \rightarrow \pi^*$ resonance are presented in Fig. 1. The combinations of the entrance and exit slit openings utilized were 50-20, 25-10, and 12.5-5 μm . The corresponding resolving powers are expected to be 5000, 10000, and 20000, respectively. It is difficult to determine the transmission function of the monochromator with the $N\ 1s \rightarrow \pi^*$ excitation of N_2 , because the natural linewidth is not well-established. This is due to the existence of several nearly overlapping vibrational bands as clearly seen in Fig. 1. However, in comparison with the recent data for the $N\ 1s \rightarrow \pi^*$ resonance of N_2 measured at Spring-8, the best energy resolution obtained might be less than 40 meV at 400 eV, which corresponds to a resolving power of more than 10000.

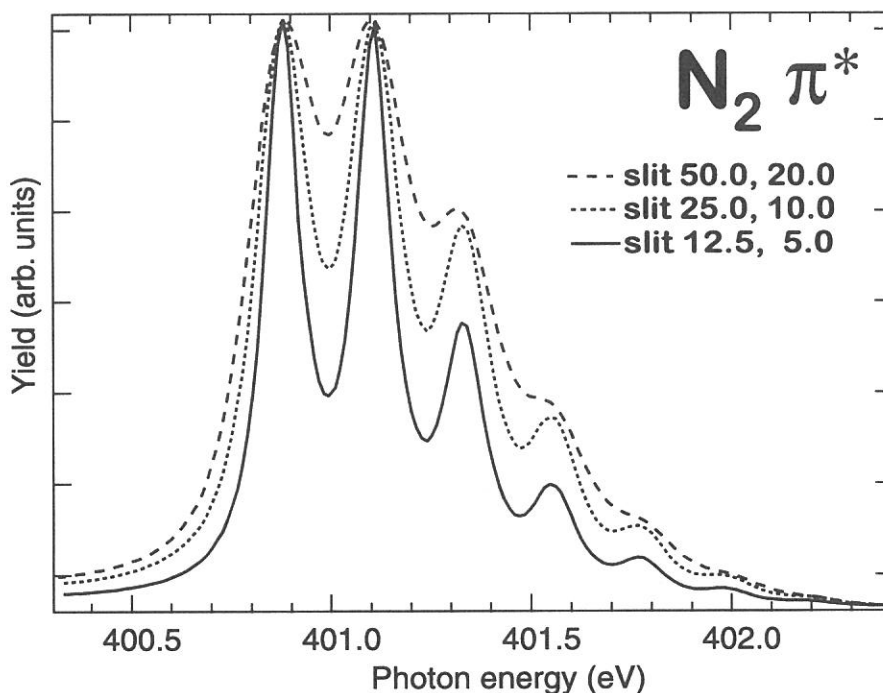


Fig. 1. High-resolution K -shell photoabsorption spectra in the π^* resonance region of N_2 .

The entrance and exit slit openings were set at 15 and 7.5 μm , which corresponds to the resolving power of 10000 at the oxygen *K*-edge region. Many fine structures due to the Rydberg excitations and their vibrational side bands are detected on the broad enhancements owing to the σ^* resonances. Due to these complicated absorption features, the estimation of the monochromator resolution from the measured spectrum is difficult in the case of O_2 . From the comparison with all available spectra of the Rydberg resonances around 530 eV, it seems possible to safely say that the resolving power obtained here is more than 5000. The estimated resolving powers for all the spectra obtained are a little worse than those expected from the numerical calculations, which may be attributable to the imperfection of the alignments of the optical elements.

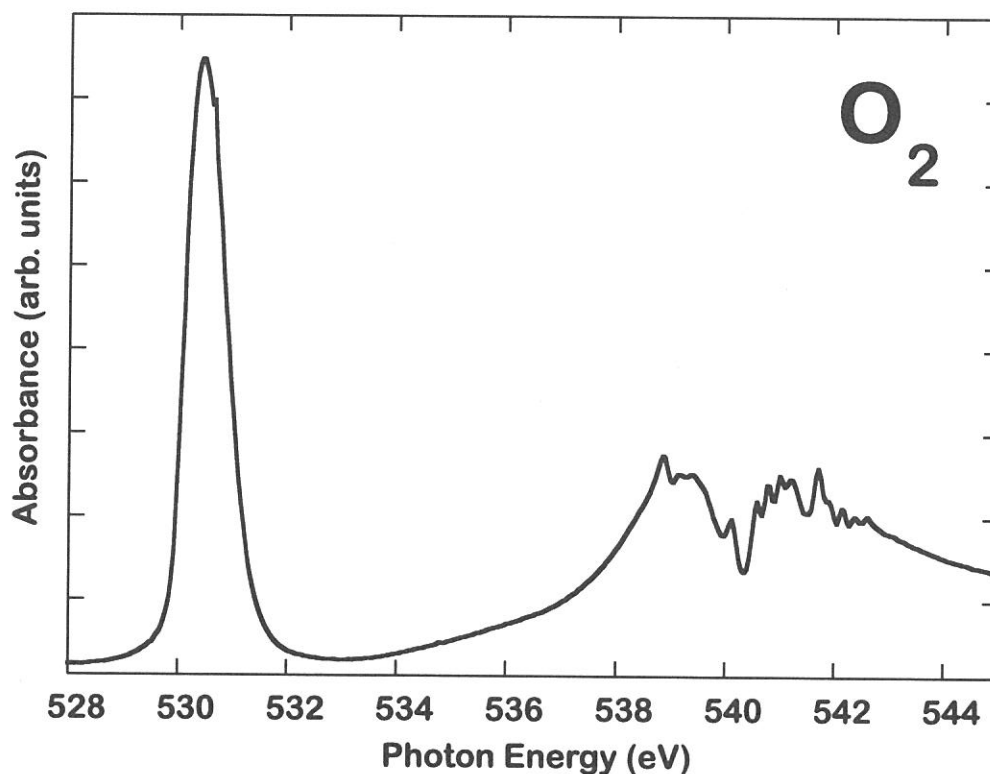


Fig. 2. *K*-shell photoabsorption spectrum of O_2 .

(BL 5A)

Experimental system for time-dependent photoelectron spectroscopy

Senku Tanaka^A, Kazutoshi Takahashi^B, Sam D Moré^B, and Masao Kamada^{A, B}

^A *The Graduate University for Advanced Studies, Myodaiji, Okazaki, 444-8585*

^B *UVSOR Facility, Institute for Molecular Science, Myodaiji, Okazaki, 444-8585*

Photoelectron spectroscopy is one of the most powerful experimental methods to investigate the electronic structures in the wide energy range. However, many experiments have been carried out by means of static way, where synchrotron radiation (SR) itself is assumed as a continuum light source like a helium lamp and an x-ray in the laboratory. These experiments use the high brilliance, continuum wavelength, polarization, cleanness of SR, and so on. On the other hand, SR has also the advantage in the temporal structure and few groups in the worldwide synchrotron radiation facilities have been trying to apply the pulse nature of the synchrotron radiation for time-dependent experiments of photoelectron spectroscopy. Moreover, the combinational use of SR and laser lights has been developing the time-dependent photoelectron spectroscopy. In this report, we present a part of our recent experimental system for temporal resolution of SR photoelectron spectroscopy.

Roughly speaking, there are two ways for the time-dependent photoelectron spectroscopy. One is the pump-probe method, where the first pulse such as laser light, electric field, pressure, and gaseous jet stimulates the material to cause remarkable changes in the electronic structures, and then the second pulse (namely, SR pulse) probes the response from the material using photoelectron spectroscopy. This pump-probe method requires the pulse nature of the SR and also the stimulation (for example, laser light), and the temporal coincidence between them. Since the UVSOR has a duration time of about 1.5 ns and a repetition of 90 MHz, this system is restricted in the temporal range of 1.5 to 11 ns under usual multi-bunch operation and can be extended to the range of 0.5 to 178 ns for a single-bunch operation. The present shortest duration of SR in the world is about few tens of pico-seconds and also the duration of few pico-seconds will be achieved in the next generation sources. Therefore time-dependent photoelectron spectroscopy using SR may attract much interest from basic researches and applications.

Another way is based on the direct measurement of the photoelectron signals decaying after the stimulation, where the fast stimulation pulse causes the change in the electronic structures of the materials and then the decaying signals following the stimulation are detected using a fast storage oscilloscope or a time-to-amplitude converter. The SR is assumed as a continuum light source and the performance of the system is restricted by the response time of the experimental system and the repetition of the stimulation. This second way is described in more details in the followings.

Experimental systems have been constructed at BL5A, UVSOR facility. Figure.1 shows the schematic block diagram of the time-dependent photoelectron spectroscopy system. We used the laser (COHERENT Mira 900-F (90 MHz, 800 nm) & RegA (10 KHz, 800 nm)) as the excited light source to cause the stimulation. The laser light was transported to the view-port of the main sample chamber using an optical fiber and focused on the sample surface using a quartz lens. SR is monochromatized by an SGM-TRAIN type monochromator and then SR photons of about 100 eV are introduced on the sample surface to observe the photoelectron spectra. The spatial overlap between laser and SR spots were carefully adjusted by the optical system of the laser. The photoelectrons are observed by an OMICRON hemi-spherical

electron-energy analyzer (EA-125HR). The electron analyzer was used in a single energy-analyzer mode. Photoelectron signals from the electron analyzer were changed to LED signals in the pre-amplifier circuit and sent to the optical receiver using an optical fiber in order to decrease the noises. Photoelectron signals acquired in the receiver were fed to the gate circuit. The gate circuit and the shutter were controlled by the timing circuit. Photoelectron signals were transferred into time-to-amplitude converters (TACs) as the start signals. Laser pulses, which were detected by a PIN photodiode, were used as the stop signals. A couple of TACs has been used to take both of laser-on/off signals, simultaneously. By changing the fixed kinetic energy, it is also possible to observe the time dependence of photoelectron spectra as well as the time-dependence of the photoelectron signals. The time-range of the present system is restricted by the response time of the system ($0.1\mu\text{s}$) and the laser repetition time ($100\mu\text{s}$). Further improvement is under progress.

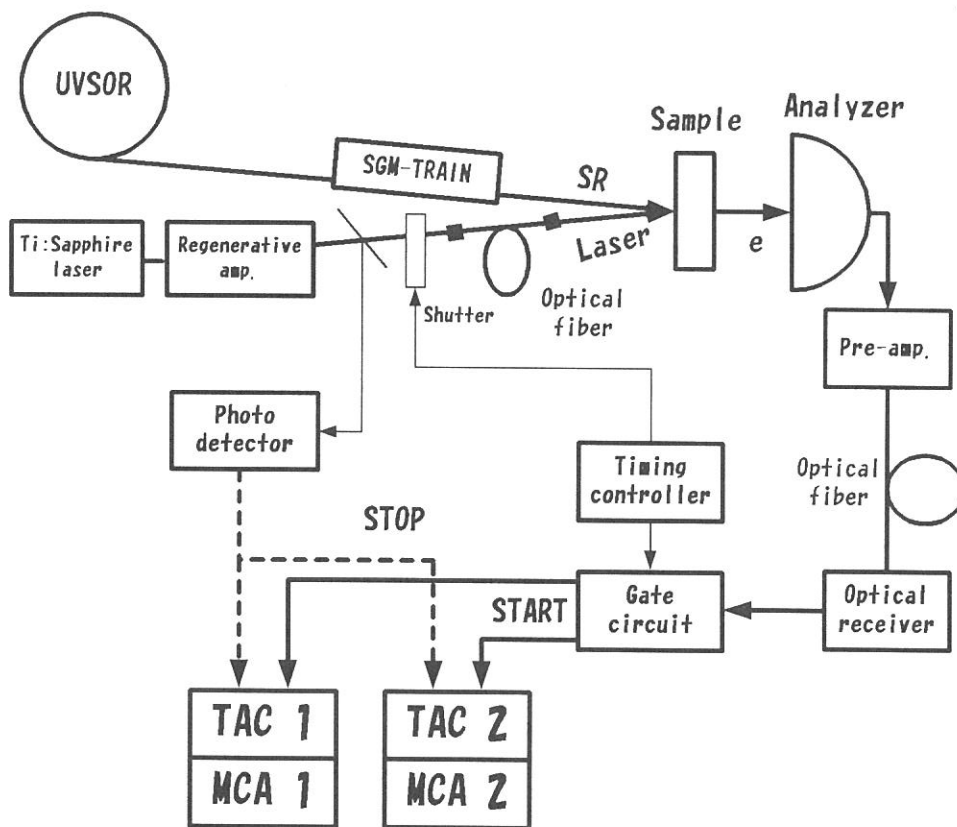


Figure 1. Schematic block diagram of the experimental system.

In summary, we have been studying the dynamical behaviors of electronic structures. We constructed the experimental system to investigate the time-dependence of the photoelectron spectra, which is based on the combinational use of the SR and laser light. The system has been applied to investigate the photo-induced phenomena on the semiconductors.

References

- [1] M. Kamada et al., *UVSOR Activity Report*, 1999, p 180.
- [2] M. Kamada et al., *Surf. Sci.*, **454-456** (2000) 525.

(BL5B)

Characterization of Optical Units and a $[\text{SnO}_2/\text{SiO}_2]_{20}$ Multilayer Spacemen for the Use of Plasma X-ray Laser Experiment

Kazumichi NAMIKAWA, RenZhong TAI, Etsuo ARAKAWA, Hisatak TAKENAKA*, Masao KAMADA**,
Masami HASUMOTO**, Eiji SHIGEMASA**

Tokyo Gakugei University, Koganei, Tokyo 184-8501

** NTT Advance Technology, Musashino, Tokyo 180-0012*

*** Institute for Molecular Science, Okazaki, Aichi 444-8584*

1. Introduction

Among existing soft x-ray sources the plasma x-ray laser is known as the most bright source; Bose degeneracy is an order of 10^9 . This means the plasma x-ray is the most suitable source to be utilized in the non-linear x-ray optical experiments. However, the plasma x-ray is a single shot source whose repetition rate, for example, at the Laser Institute of Osaka University is 1 shot per two hours. Prior to the plasma x-ray laser experiment, we obliged to characterize the spacemen and the optical units, and to prepare an off beam alignment of these materials. We report here the results of the experiments characterized a two axis goniometer and a $[\text{SnO}_2/\text{SiO}_2]_{20}$ multilayer spacemen which we fabricated for Ni-like Ag plasma x-ray laser experiment; stimulated x-ray parametric scattering (SXPS).

2. Experimental

A new-designed goniometer, which consists of an entrance slit, a sample and an exit slit closely attached by a silicon photodiode, as shown in Figure 1, was installed in the scattering chamber at BL-5B. The design parameters of this sample are a multilayer period at 10 nm with a thickness of top layer SnO_2 at 2 nm, a number of periods at 20, and a substrate of SiO_2 . The widths of the two slits were set to 1 mm. The change of the photon energy is given by the monochromator of the beam line.

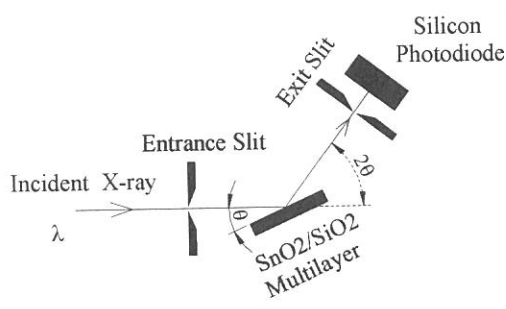


Fig. 1 Experimental set-up

3. Results and Discussion

Bragg reflections were measured for various wave lengths. Figure 2 shows a typical Bragg reflection of the

sample, with a peak reflectance estimated at 10% and a FWHM at around 5° due to the finite number of layers.

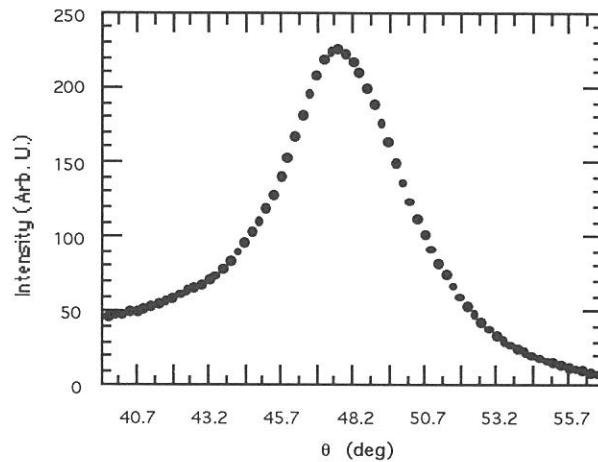


Fig. 2 Bragg reflection for the $[\text{SnO}_2/\text{SiO}_2]_{20}$ multilayer. The incident x-ray wave length is 14.437 nm, the peak appears at 47.63 degree.

The broad tail of Fig. 2 will inevitably contribute a background noise to the SXPS with this sample. This influence was measured as shown in Fig. 3 by 2-theta scanning, with the theta set at 55.36° , which is the designed value of SXPS. At the signal direction, a background was measured to be with magnitude of 0.38% of the peak Bragg reflection.

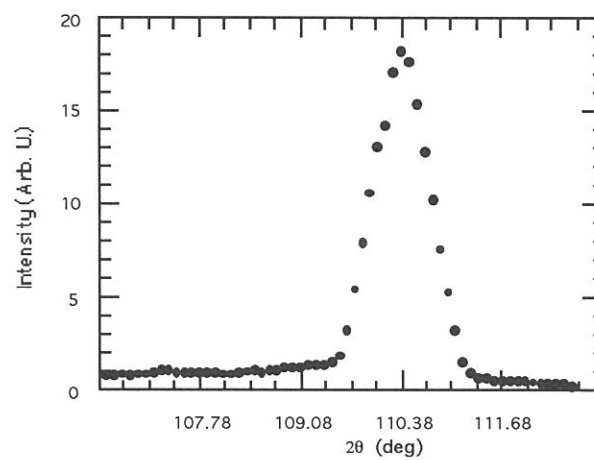


Fig. 3 Background from the tail of specular reflection. The peak arises from the broad tail of Bragg reflection as shown in Fig. 2. The SXPS signal is expected to appear -3.74° off this peak.

A clear N_3 , N_4 absorption edge of Sn^{4+} was also observed by measuring the reflected intensities for different incident photon energies. This is a good verification of the transition between 4p and the lower edge of 5d-conduction band of Sn^{4+} , which has been presumed to exist in the process of SXPS.

(BL5B)

Measurement of SELENE/UPI-TEX FM mirror reflectivity

Masato Nakamura^A, Tetsunori Murachi^A, Ichiro Yoshikawa^B,
Atsushi Yamazaki^A, Kei Shiomi^A and Yoshiyuki Takizawa^C

^A*Department of Earth and Planetary Science, University of Tokyo, Bunkyo-ku, Tokyo 113-0033,
Japan*

^B*Institute of Space and Astronautical Science, Sagamihara, Kanagawa 229-8510, Japan*

^C*The Institute of Physical and Chemical Research, Wako, Saitama 351-0198, Japan*

As one of the calibrations for the reflectivity characteristics of the multi-layer coated mirror (UPI (Upper-atmosphere and Plasma Imager)-TEX (Telescope of EXtreme ultra-violet) FM (Flight Model) mirror) for the Lunar orbiter SELENE (SELenological and ENgineering Explorer), the purpose of this experiment is to measure the reflectivity of multi-layered mirror at different areas and different incident angles.

The UPI-TEX on board SELENE will measure the abundance and distribution of Helium gas and ions in the Terrestrial Plasmasphere. Neutral Helium gas scatter the 58.4nm (He I emission) and those ions scatter 30.4nm (He II emission) Extreme Ultra-Violet (EUV) light from the sun which are the target of this telescope. Mo/Si multi-layered mirror reflects preferentially 30.4nm EUV light.¹⁾ Maximum reflectivity that peaks at 30.4nm is about 24% and the full width at half of maximum is about 4nm. The reflectivity above 50nm again increases. This type of mirror was used in the Helium Emission Monitor (HEM) boarded on the sounding rocket S-520-19²⁾, eXtreme Ultra-Violet (XUV) Scanner boarded on the Mars orbiter NOZOMI^{3,4)} (Fig.1) and will be SELENE.

Below is why we measure the reflectivity of multi-layered mirror at different areas and different incident angles. As shown in Fig.1, the black line and the gray line, which come from different directions, are reflected by different incident angles at same mirror area, and are detected at different areas of MicroChannel Plates (MCPs). As it is well known that the reflectivity depends on incident angles, the light reflected at same area by different incident angles, which originally have same intensity, are measured at different intensity by MCPs. And by the curvature of mirror the light, which from same direction and reflected at different mirror areas are reflected to same MCPs area, result in different intensity. In brief, the 2D-intensity-distributions detected by MCPs may differ from TRUE 2D-intensity-distributions of light from the objects.

To measure the reflectivity of multi-layered mirror at different areas and different incident angles we did below. We got the pure EUV light free from the contamination of multi-order light.⁵⁾ We fixed the mirror that the frame plane of mirror was perpendicular to beam line and the center of mirror corresponded to beam line. We decided measurement points: (r, i) = (30, 6.5), (40, 5.0), (40, 6.5), (50, 3.2), (50, 5.0), (50, 6.5), where r is the distances [mm] at the measurement point from the mirror center, i is the incident angles [degree] (6.5 degrees are corresponding to a 6.5-degree half

field of view). We injected XUV light to measurement points of mirror, and measured the reflectivity of the multi-layered mirror.

The result is shown in Fig.2. The large (small) markers have less error than 10% (20%) of reflectivity. It is ascertained that this multi-layered mirror reflects preferentially 30.4nm XUV light. The reflectivity above 50nm again increases. The reflectivity varies with incident angles: at 30.4nm in Fig.2 (a), (b) the reflectivity of 5.0 degrees differs from that of 6.5 degrees significantly. This result implies that the reflectivity of 0.0 degrees might have remarkable difference from that of 5.0 degrees. Because this mirror designed at 0.0-degree incident angle, this thought must be ascertained. We will measure the reflectivity characteristics of 0.0~6.5 degrees and different areas in detail.

References

- 1) T. Yamazaki et al., *J. Electron Spectrosc. Relat. Phenom.*, 80, 229, 1996.
- 2) I. Yoshikawa et al., *J. Geophys. Res.*, 102, 19897, 1997.
- 3) M. Nakamura et al., *Earth, Planets and Space*, 51, 61, 1999.
- 4) M. Nakamura et al., *Geophys. Res. Lett.*, 27, 141, 2000.
- 5) M. Nakamura et al., *UVSOR Activity Report*, 152, 1998.

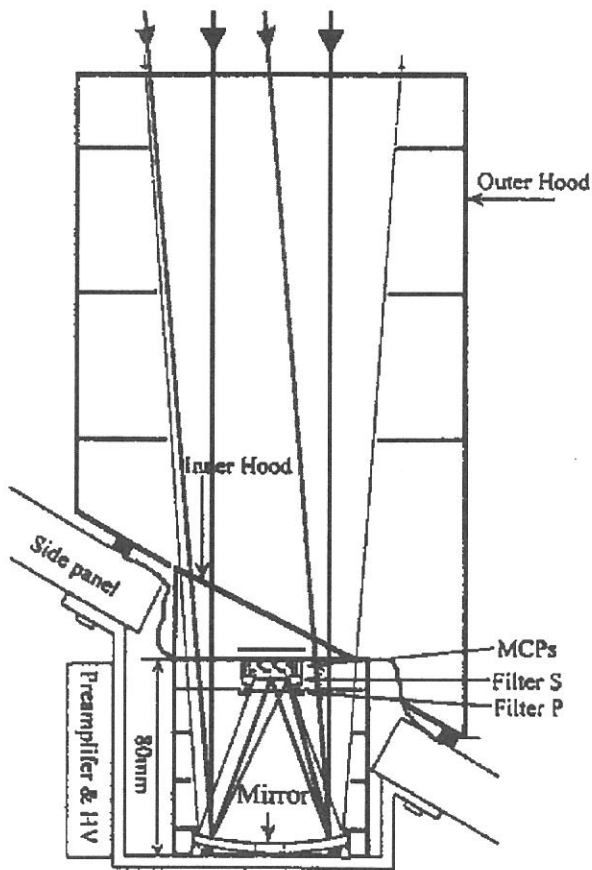


Fig.1 A cross section of the XUV scanner on board the Mars orbiter NOZOMI.

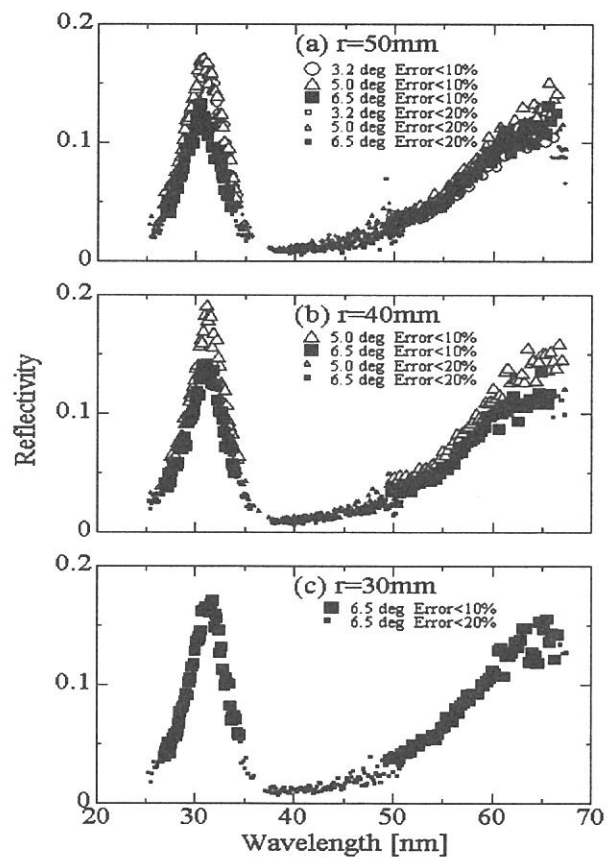


Fig.2 Reflectivity characteristics of UPI-TEX FM mirror for the Lunar orbiter SELENE at (a) r=50mm (b) r=40mm (c) r=30mm from mirror center.

(BL-5B)

Charge Spreading in Back Illuminated CCD

Ryouhei KANO¹, Kazuyoshi KUMAGAI¹, Tomonori TAMURA¹, Saku TSUNETAI¹,
Taro SAKAO², Yukio KATSUKAWA³

¹ National Astronomical Observatory, 2-21-1 Osawa, Mitaka, Tokyo 181-8588, Japan

² The Institute of Space and Astronautical Science, 3-1-1 Yunodai, Sagamihara, Kanagawa 229-8510, Japan

³ Department of Astronomy, School of Science, The University of Tokyo, Bunkyo, Tokyo 113-0033, Japan

A cloud of electrons generated by an incident X-ray in a CCD are dispersed, while they travel to electrodes on the CCD surface. If these electrons spread out of a CCD pixel, the image taken with the CCD is blurred.

We investigated the charge spreading in a commercial-based back-illuminated CCD device developed by Marconi Applied Technologies (MAT): CCD42-40, by utilizing beam lines located at UVSOR Facility in Okazaki National Research Institute and Photon Factory in High Energy Accelerator Research Organization. The same type of the CCD will be used for the X-ray Telescope (XRT) aboard the Solar-B satellite, which will be launched in summer of 2005.

In order to obtain the CCD spatial response with sub-pixel resolution, we used the mesh technique which was developed by Tsunemi et al. (1997). We prepared a copper mesh whose pinhole is $4\mu\text{m}$ in diameter, and whose pitch length is twice larger than the CCD pixel size ($13.5\mu\text{m}$). Just in front of a test CCD, we put the mesh, and rotated it by a few degree around the normal of the CCD surface. The moire pattern clearly appears in raw images (Fig.1). Because of its geometrical regularity, it is easy to derive the relative position of each pixels from pinholes of the mesh. Figure 2 shows the intensity distribution based on the mesh coordinates. The electrons generated by X-ray photons passing through a pinhole located at (1.5, 1.5) spread out of a pixel (bashed box). The modulation pattern is blurred not only by the charge spreading in a CCD but also by the diffraction of a pinhole. We, therefore, subtracted the effect of the diffraction. We approximated the distribution of the charge spreading in CCD 42-40 by a Gaussian function, and then plotted its standard deviation as a function of the absorption depth in silicon at the measured wavelengths (Fig. 3). Because X-ray photons with the shorter wavelength penetrate closer to the electrodes at the front surface, we expected that the shorter wavelength made the smaller spreading size. However, we also expected that the dependence of the spreading size on the absorption depth might be small, because most of X-ray photons are absorbed near the back surface even in the case of the shorter wavelength. In fact, Figure 3 shows the size is almost constant around 0.5 pixel ($6.25\mu\text{m}$), except for the data at 100\AA . The constant spreading size may be a general character of back-illuminated CCDs.

As a practical point of view, this experiment shows that the charge spreading in MAT CCD42-40 is one of

the primary factors for the image blurring. In fact, we have to pay attention to the charge spreading as well as the optical aberrations and the spacecraft jitter, to evaluate the spatial resolution of XRT.

We would like to thank Prof. Tsunemi and his colleagues of Osaka University for supporting this experiment based on their mesh technique.

References:

Tsunemi, Yoshita & Kitamoto 1997, Jpn. J. Appl. Phys., Vol.36, pp2906-2911

Fig. 1.. A part of a raw image, which shows the clear moire pattern produced by pinholes of the mesh and CCD pixels.

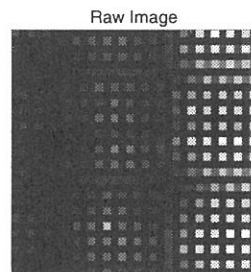


Fig. 2.. The normalized intensity distribution shown on the mesh coordinated. Pinholes are located at (1.5, 1.5), (1.5, 3.5), (3.5, 1.5) and (3.5, 3.5).

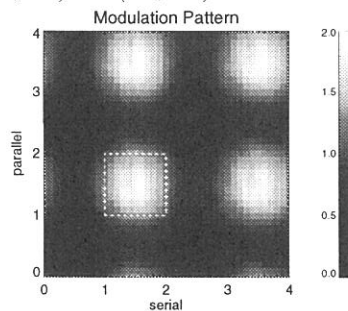
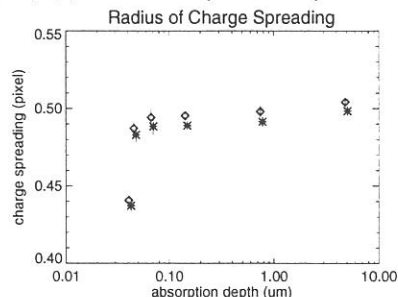


Fig. 3.. The standard deviation of the charge spreading in CCD42-40 along the serial (stars) and parallel (diamonds) resistors, as a function of the absorption depth in silicon. The data points correspond to the measured wavelengths; 100, 80, 60, 40, 20 and 10 \AA from the left.



(BL8A)

Study of the carbon contamination of the SR irradiated optical devices

Takashi Naito, Mikio Tadano, Junji Urakawa,¹
Eiken Nakamura, Masami Hasumoto,²

¹High energy Accelerator research organization(KEK),
Accelerator Division,1-1 Oho Tsukuba 305-0801, Japan
²Institute of Molecular Science, Okazaki 444-8585, Japan

A carbon contamination of the optical devices is a serious problem for the operation of synchrotron radiation beam lines(SR-BL) and for the measurements by the optical monitors of the accelerator. From the experience of the SR-BL, we had to replace the gratings or the mirrors after several operation periods. From the experience of the SR interferometer of Accelerator Test Facility in KEK(ATF-KEK), the carbon contamination for the visible light of the first mirror has limited the resolution of the beam size measurement. The purpose of this study is to find out the dependence of the growth rate of the carbon contamination and to investigate the key parameter for keeping the clean mirror surface.

In order to investigate the growth rate of the carbon contamination, the experiments were carried out at BL8A. The growth rate of the carbon contamination was measured with a reflected light power of 670nm laser light at different conditions. The measurement set up is shown in fig. 1. The optical mirror(BK7, Aluminum+MgF2 coated) was used as a test sample. The reflected laser power was measured by PIN Photo Diodes(Hamamatsu S3590). Two photo diodes were used to compare the reflection of the SR irradiated part and the normal part. Fig. 2 shows the reflectivity as a function of dose(time x current) in two cases of mirror temperature of 25 degrees and 100 degrees, respectively. The clearly temperature dependence of the carbon contamination was measured. For the more, the series of the study is scheduled at various conditions.

References

- [1] K. Bollner et. al., "INVESTIGATION OF CARBON CONTAMINATION OF MIRROR SURFACES EXPOSED OT SYNCHROTRON RADIATION" DESY SR-82-18 Oct. 1982
[2] A. Kumao et. al., " Study on Specimen Contamination by Transmission Electron Microscopy", J. Electron Microsc., Vol 30, No.3, 161-170

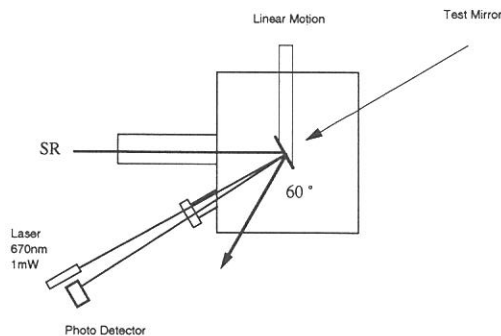


Fig.1 Measurement setup:

The incident SR is reflected with high angle (60degrees).
The reflectivity of the mirror of the irradiated position is measured by 670nm laser.

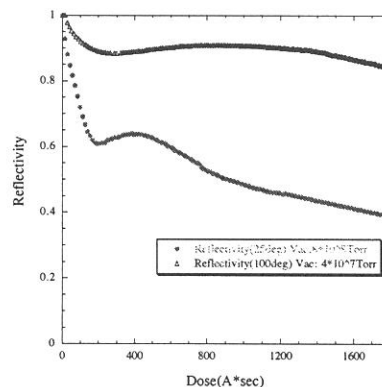


Fig.2 Reflectivity as a function of dose for different temperature.

(BL6A2)

Beamline Upgrade for Photoelectron Microscopy with the Combination of Synchrotron Radiation and Laser

Kazutoshi Takahashi^A, Yoichiro Doi^B, Kazutoshi Fukui^C, Yuichi Haruyama^D,
Toyohiko Kinoshita^E, and Masao Kamada^A

^A*UVSOR Facility, Institute for Molecular Science, Okazaki 444-8585*

^B*Faculty of Engineering, Fukui University, Fukui 910-8507*

^C*VUV Photo-Science, Institute for Molecular Science, Okazaki 444-8585*

^D*LASTI, Himeji Institute for Technology, Ako 678-1201*

^E*ISSP, University of Tokyo, Kashiwa 277-8581*

Photoelectron spectroscopy is one of the most powerful techniques to investigate the electronic structures of various materials. BL6A2 has been used for the photoemission study for solids and surfaces using the home-made angle-integrated and angle-resolved photoelectron spectrometers for more than 10 years. However, it has been suggested that these spectrometers should be replaced by newer one due to their poor resolution and low efficiency on collecting data. Recently, various photo-induced phenomena such as the electronic non-equilibrium on the photo-excited semiconductor surface, photo-induced phase transition on transition metal complexes has been attracting much interest. The combinational use of the synchrotron radiation and laser is attractive and promising, since it is powerful to investigate the various photo-induced phenomena. Moreover, newly developed photoelectron micro-spectroscopic method has many applied usages compared with ordinary one, because it can measure the specific small area of the sample. In this report, we present the new experimental system for photoelectron micro-spectroscopy with the combination of synchrotron radiation and laser.

Figure 1 shows the schematic view of the upgraded BL6A2. In order to connect the photoelectron micro-spectroscope (FISIONS Instruments, ESCALAB 220i-XL) to the plane grating monochromator, a post-mirror M3 was replaced by plane mirror and a new post-mirror M4 was installed. M4 is a toroidal mirror with the radius of $R_h = 4266.3$ mm and $R_v = 446.9$ mm. These parameters have been determined to minimize the beam size at the sample by raytrace simulation. Figure 2(a) shows the beam spot at the sample obtained from the raytrace simulation. The photoelectron micro-spectroscope has been installed at the focusing point of the monochromized light. The laser light from the cw Ar⁺ ion laser, Nd:YAG laser with the pulse width of 300 ps, and Ti:Sapphire laser with the pulse width of 100 fs can be introduced through the quartz view-port of the main sample chamber. The base pressure of the analyzing chamber is about 2×10^{-8} Pa. The samples can be cooled with a flow-type He cryostat. The sample preparation chamber equipped with a load-lock chamber is connected to the main sample chamber.

The photon flux at the sample determined by the total electron yield of Au sample is about 6×10^{10} photons/sec/100mA at $h\nu = 60-100$ eV and the slit width of 100 μm . Figure 2(b) shows the

beam spot measured by the photoelectron imaging for valence band of Cu sample at $h\nu = 100$ eV. As shown in Fig 2(a), the beam size at the sample is about 0.5 mm in diameter, which is almost same as that of raytrace simulation. Total instrumental energy resolution is 0.1-0.2 eV, dependent on the photon energy. The spatial resolution was determined by the photoelectron imaging for the C 1s core-level from knife-edge sample excited by Mg $K\alpha$ line. The spatial resolution were about 8 and 6 μm for the measuring area of 1.0×1.0 and 0.5×0.5 mm^2 , respectively.

In summary, the new experimental system for photoelectron micro-spectroscopy with the combination of synchrotron radiation and laser has been constructed at beamline BL6A2. Using this system, photoelectron spectro-microscopic studies of various photo-induced phenomena can be conducted.

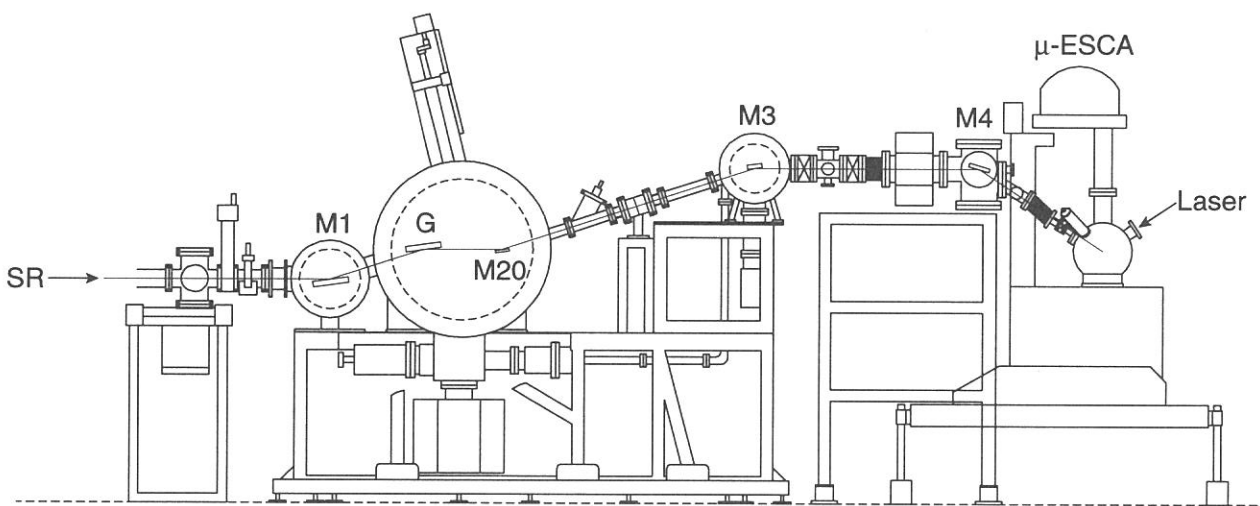


Fig. 1 Schematic view of the upgraded BL6A2.

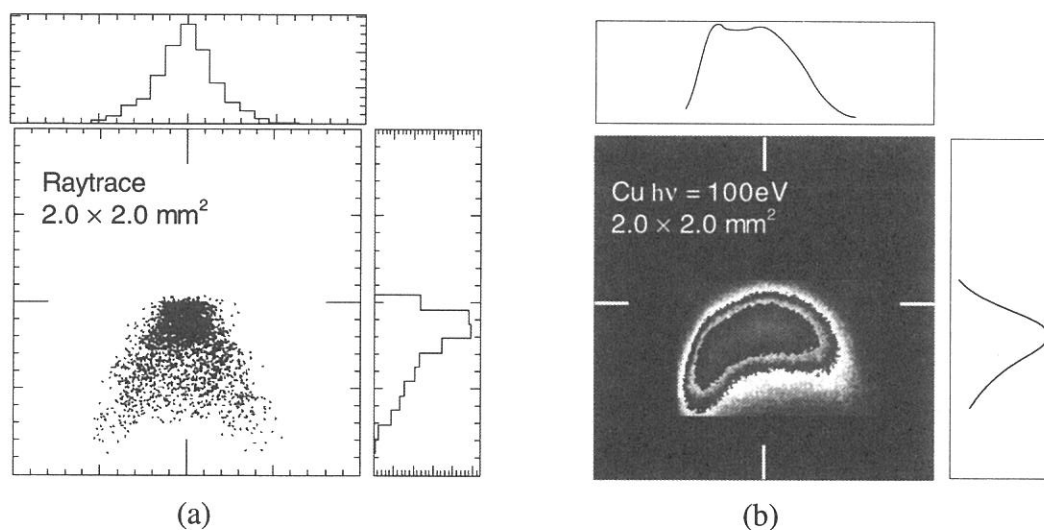


Fig. 2 The beam spot at the sample determined by (a) raytrace simulation and (b) photoelectron imaging for gold sample at $h\nu = 100$ eV.

(BL8B1)

Development of Siegbahn-type coaxially symmetric mirror electron energy analyzer for photoemission and electron-ion coincidence spectroscopy in gas phase

Koji Isari, Kenichiro Tanaka, Masaki Morita, Yasumitsu Suto, Hiroaki Yoshida, Kazuhiko Mase,^A Tatsuo Gejo,^B Shin-ichi Nagaoka^B

Department of Physics Science, Faculty of Science, Hiroshima University, 1-3-1 Kagamiyama, Higashi-Hiroshima 739-8527

^A*Photon Factory, Institute of Materials Structure Science, High Energy Accelerator Research Organization, 1-1 Oho, Tsukuba 305-0801,*

^B*Institute for Molecular Science, Myodaiji Okazaki 444-8585*

Coincidence method is one of the most powerful tools for investigating ionization process, dissociation dynamics and auger decay process. We have developed a coaxially symmetric mirror electron energy analyzer proposed by Kai Siegbahn et al.[1] for photoemission spectroscopy and electron-ion coincidence spectroscopy in gas phase. Figure 1 shows a schematic diagram of the analyzer. It consists of inner and outer electrodes, five sets of electrodes for maintaining a coaxial electric field, a 0.8-mm-diameter exit slit and tandem micro channel plates (MCP), a magnetic shield, a 203-mm-diameter conflat flange with feedthroughs, and an xyz stage for position adjustment. The solid angle of the analyzer is designed to be 1.2sr. The performance of the analyzer was examined by measuring resonant Auger spectrum of N_2 at BL-8B1. Synchrotron radiation was cut by a pin hole with a diameter of 1 mm to reduce the ionization area of sample. The N_2 pressure at the experimental chamber was kept at 5×10^{-6} Torr. Figure 2 shows a resonant Auger electron spectrum of N_2 at $\pi^* \leftarrow 1s$. The energy resolution was estimated as $E/\Delta E = 110$ at the $3\sigma_g^{-1}$ peak, which is twice better than that of a cylindrical mirror analyzer (CMA) which was used before at BL-8B1. The brilliance of the analyzer, however, was one order of magnitude poorer than that of CMA, because the ionization area of the N_2 is much larger than the exit slit area of the analyzer. Energy resolution and brilliance will be improved with a suitable slit in future.

References

[1] K. Siegbahn et al., *Nucl. Instr. and Meth. in Phys. Res. A384*, 563-574 (1997).

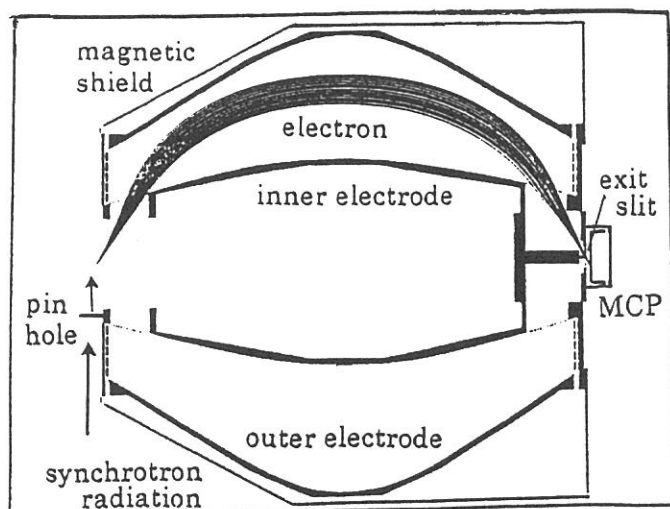


Figure 1. Schematic drawing of the Siegbahn-type coaxially symmetric mirror electron energy analyzer.

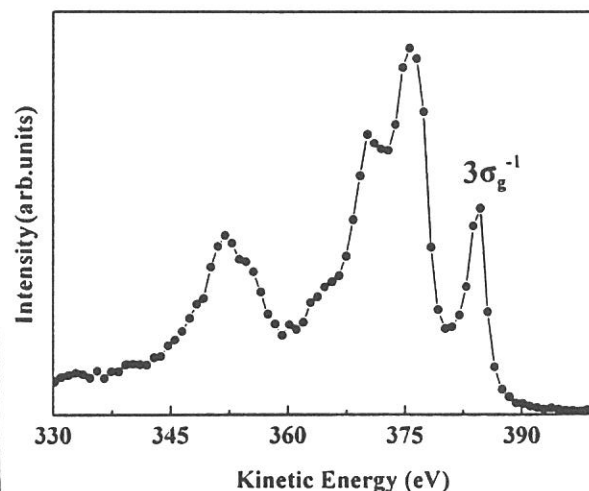


Figure 2. Resonant Auger electron spectrum of N_2 at $\pi^* \leftarrow 1s$.